

Four-nucleon shell-model calculations in a Faddeev-like approach

P. Navrátil* and B. R. Barrett

Department of Physics, University of Arizona, Tucson, Arizona 85721

(Received 25 August 1998)

We use equations for Faddeev amplitudes to solve the shell-model problem for four nucleons in a model space that includes up to $14\hbar\Omega$ harmonic-oscillator excitations above the unperturbed ground state. Two- and three-body effective interactions derived from the Reid93 and Argonne V8' nucleon-nucleon potentials are used in the calculations. Binding energies, excitation energies, point-nucleon radii, and electromagnetic and strangeness charge form factors for ${}^4\text{He}$ are studied. The structure of the Faddeev-like equations is discussed and a formula for the matrix elements of the permutation operators in a harmonic-oscillator basis is given. The dependence on harmonic-oscillator excitations allowed in the model space and on the harmonic-oscillator frequency is investigated. It is demonstrated that the use of three-body effective interactions improves the convergence of the results. [S0556-2813(99)03004-6]

PACS number(s): 21.45.+v, 21.60.Cs, 21.30.Fe, 27.10.+h

I. INTRODUCTION

Many different methods have been used to solve the few-body problem in the past. One of the most viable approaches appears to be the Faddeev method [1]. It has been successfully applied to solve the three-nucleon bound-state problem for various nucleon-nucleon potentials [2–6]. For solution of the four-nucleon problem one can employ Yakubovskii's generalization of the Faddeev formalism [7] as done, e.g., in Ref. [8]. Alternatively, other methods have also been successfully used in the past, such as the Green's function Monte Carlo (GFMC) method [9] and the correlated hyperspherical harmonics expansion method [10].

On the other hand, when studying the properties of more complex nuclei one typically resorts to the shell model. In that approach, the harmonic-oscillator basis is used in a truncated model space. Instead of the free nucleon-nucleon potential, one utilizes effective interactions appropriate for the truncated model space. Examples of such calculations are the large-basis no-core shell-model calculations that have recently been performed [11,12]. In these calculations all nucleons are active, which simplifies the effective interaction as no hole states are present. The effective interaction is determined for a system of two nucleons in a harmonic-oscillator well interacting by the nucleon-nucleon potential and is subsequently used in many-particle calculations.

In a recent paper we combined the shell-model approach to the three-nucleon problem with the Faddeev formalism [13]. That allowed us to extend the shell-model calculations to a model space of excitations of $32\hbar\Omega$ above the unperturbed ground state and to study the convergence with respect to the size of the model space. In the present paper we generalize these earlier calculations to the four-nucleon problem. We introduce equations for Faddeev amplitudes that are fully antisymmetrized for three nucleons. As the center-of-mass term is removed, we are able to work in a model space up to an excitation of $14\hbar\Omega$ above the unperturbed ground state. For comparison the largest shell-model calculations so

far for ${}^4\text{He}$ are those performed by Ceuleneer *et al.*, in which a $10\hbar\Omega$ model space was utilized [14]. The main motivation for the present work is to test the shell-model approach and the effective interactions derived from realistic nucleon-nucleon (NN) potentials that are used in conventional shell-model applications for more complex systems. As the equations that we employ can be conveniently used with three-body interactions or three-body effective interactions, we investigate, in addition to two-body effective interactions, also three-body effective interactions in the present formalism. Such effective interactions are not typically used in traditional applications. We show that the inclusion of three-body effective interactions improves the overall convergence of the results. At the same time our work serves as an alternative method to solving the four-nucleon problem. We can study the convergence properties of the results with increasing size of the model space. If convergence is achieved, our results will approach the exact solutions obtained by other methods. In our formalism we seek simultaneously solutions for both the ground state and the excited states. In the past, the variational Monte Carlo method was used to investigate the excited states of ${}^4\text{He}$ using realistic NN potentials [15]. In most four-nucleon calculations with realistic NN potentials, however, only the ground-state properties were evaluated [8,10]. On the other hand, earlier studies that investigated excited-state properties usually did not employ realistic NN potentials [14,16]. Recently, the four-nucleon resonant and scattering states were investigated using realistic NN potentials in the framework of the resonating group method [17] and the correlated-hyperspherical-harmonics method [18] as well as in the solution of the Faddeev-Yakubovskii equations in configuration space [19].

The present calculation is simplified by using a compact formula for the matrix elements of the permutation operators in the harmonic-oscillator (HO) basis. Also, because of the way we do the model-space truncation, we keep the equivalence of the Faddeev-like and Schrödinger equations throughout the calculation. In addition to calculation of ground-state and excited-state energies and point-nucleon rms radii, we also evaluate electromagnetic (EM) and strangeness form factors in the impulse approximation.

In Sec. II we first discuss the Faddeev equations for the

*On leave of absence from the Institute of Nuclear Physics, Academy of Sciences of the Czech Republic, 250 68 Řež near Prague, Czech Republic.

shell-model problem of three nucleons. Then a generalization to the four-nucleon system is introduced. In Sec. III we present the energy, radii, and form factor results for ${}^4\text{He}$. Conclusions are given in Sec. IV.

II. SHELL MODEL AND FADDEEV-LIKE FORMALISM

In shell-model studies the one- plus two-body Hamiltonian for the A -nucleon system, i.e.,

$$H = \sum_{i=1}^A \frac{\vec{p}_i^2}{2m} + \sum_{i<j}^A V_N(\vec{r}_i - \vec{r}_j), \quad (1)$$

where m is the nucleon mass and $V_N(\vec{r}_i - \vec{r}_j)$ is the NN interaction, is usually modified by adding the center-of-mass HO potential $\frac{1}{2}Am\Omega^2\vec{R}^2$, $\vec{R} = (1/A)\sum_{i=1}^A\vec{r}_i$. This potential does not influence the intrinsic properties of the many-body system. It provides, however, a mean field felt by each nucleon and allows us to work with a convenient HO basis. The modified Hamiltonian, depending on the HO frequency Ω , can be cast into the form

$$H^\Omega = \sum_{i=1}^A \left[\frac{\vec{p}_i^2}{2m} + \frac{1}{2}m\Omega^2\vec{r}_i^2 \right] + \sum_{i<j}^A \left[V_N(\vec{r}_i - \vec{r}_j) - \frac{m\Omega^2}{2A}(\vec{r}_i - \vec{r}_j)^2 \right]. \quad (2)$$

The one-body term of the Hamiltonian (2) can be rewritten as a sum of the center-of-mass term, $H_{\text{c.m.}}^\Omega = \vec{P}_{\text{c.m.}}^2/2Am + \frac{1}{2}Am\Omega^2\vec{R}^2$, where $\vec{P}_{\text{c.m.}} = \sum_{i=1}^A\vec{p}_i$ and a term depending only on the relative coordinates. In the present application we use a basis which explicitly separates center-of-mass and relative-coordinate wave functions. Therefore, the contribution of the center-of-mass term is trivial and will be omitted from now on.

The shell-model calculations are performed in a finite model space. Therefore, the interaction term in Eq. (2) must be replaced by an effective interaction. In general, for an A -nucleon system, an A -body effective interaction is needed. In practice, the effective interaction is usually approximated by a two-body effective interaction. In the present study we will also employ a three-body effective interaction. As approximations are involved in the effective interaction treatment, large model spaces are desirable. In that case, the calculation should be less affected by any imprecision of the effective interaction. The same is true for the evaluation of any observable characterized by an operator. In the model space, renormalized effective operators are required. The larger the model space, the less renormalization is needed. We may take advantage of the present approach to perform shell-model calculations in significantly larger model spaces than are possible in the conventional shell-model approach. At the same time we can investigate the convergence properties of effective interactions.

A. Three-nucleon system

In this subsection we repeat the steps discussed in Ref. [13] that are needed to solve the three-nucleon shell-model problem in the Faddeev formalism. For a three-nucleon system, i.e., $A=3$, a transformation of the coordinates,

$$\vec{r} = \sqrt{\frac{1}{2}}(\vec{r}_1 - \vec{r}_2), \quad (3a)$$

$$\vec{y} = \sqrt{\frac{2}{3}} \left[\frac{1}{2}(\vec{r}_1 + \vec{r}_2) - \vec{r}_3 \right], \quad (3b)$$

and, similarly, of the momenta, can be introduced that brings the relative-coordinate part of the one-body HO Hamiltonian into the form

$$H_0 = \frac{\vec{p}^2}{2m} + \frac{1}{2}m\Omega^2\vec{r}^2 + \frac{\vec{q}^2}{2m} + \frac{1}{2}m\Omega^2\vec{y}^2. \quad (4)$$

Eigenstates of this Hamiltonian,

$$|nlsjt, \mathcal{N}\mathcal{L}\mathcal{J}, JT\rangle, \quad (5)$$

are then used as the basis for the three-nucleon calculation. Here n, l and \mathcal{N}, \mathcal{L} are the HO quantum numbers corresponding to the harmonic oscillators associated with the coordinates and momenta \vec{r}, \vec{p} and \vec{y}, \vec{q} , respectively. The quantum numbers s, t , and j describe the spin, isospin, and angular momentum of the relative-coordinate partial channel of particles 1 and 2, while \mathcal{J} is the angular momentum of the third particle relative to the center of mass of particles 1 and 2. The J and T are the total angular momentum and the total isospin, respectively.

The Faddeev equation for the bound system can be written in the form

$$\tilde{H}|\phi\rangle = E|\phi\rangle, \quad (6)$$

with

$$\tilde{H} = H_0 + V(\vec{r})\mathcal{T}. \quad (7)$$

Here, $V(\vec{r}) = V_N(\sqrt{2}\vec{r}) - (1/A)m\Omega^2\vec{r}^2$ is the potential and \mathcal{T} is given by

$$\mathcal{T} = 1 + \mathcal{T}^{(-)} + \mathcal{T}^{(+)}, \quad (8)$$

with $\mathcal{T}^{(+)}$ and $\mathcal{T}^{(-)}$ the cyclic and the anticyclic permutation operators, respectively. Previously [13], we derived a simple formula for the matrix elements of $\mathcal{T}^{(-)} + \mathcal{T}^{(+)}$ in the basis (5), namely,

$$\begin{aligned}
& \langle n_1 l_1 s_1 j_1 t_1, \mathcal{N}_1 \mathcal{L}_1 \mathcal{J}_1, JT | \mathcal{T}^{(-)} + \mathcal{T}^{(+)} | n_2 l_2 s_2 j_2 t_2, \mathcal{N}_2 \mathcal{L}_2 \mathcal{J}_2, JT \rangle \\
&= -\delta_{N_1, N_2} \sum_{LS} \hat{L}^2 \hat{S}^2 \hat{j}_1 \hat{j}_2 \hat{\mathcal{J}}_1 \hat{\mathcal{J}}_2 \hat{s}_1 \hat{s}_2 \hat{t}_1 \hat{t}_2 (-1)^L \begin{Bmatrix} l_1 & s_1 & j_1 \\ \mathcal{L}_1 & \frac{1}{2} & \mathcal{J}_1 \\ L & S & J \end{Bmatrix} \begin{Bmatrix} l_2 & s_2 & j_2 \\ \mathcal{L}_2 & \frac{1}{2} & \mathcal{J}_2 \\ L & S & J \end{Bmatrix} \begin{Bmatrix} \frac{1}{2} & \frac{1}{2} & s_1 \\ \frac{1}{2} & S & s_2 \end{Bmatrix} \begin{Bmatrix} \frac{1}{2} & \frac{1}{2} & t_1 \\ \frac{1}{2} & T & t_2 \end{Bmatrix} \\
& \times [(-1)^{s_1+s_2+t_1+t_2-L_1-L_2} \langle \mathcal{N}_1 \mathcal{L}_1 n_1 l_1 L | n_2 l_2 \mathcal{N}_2 \mathcal{L}_2 L \rangle_3 + \langle n_1 l_1 \mathcal{N}_1 \mathcal{L}_1 L | \mathcal{N}_2 \mathcal{L}_2 n_2 l_2 L \rangle_3], \tag{9}
\end{aligned}$$

where $N_i = 2n_i + l_i + 2\mathcal{N}_i + \mathcal{L}_i$, $i = 1, 2$, $\hat{j} = \sqrt{2j+1}$, and $\langle \mathcal{N}_1 \mathcal{L}_1 n_1 l_1 L | n_2 l_2 \mathcal{N}_2 \mathcal{L}_2 L \rangle_3$ is the general HO bracket for two particles with mass ratio 3 as defined, e.g., in Ref. [20]. Expression (9) can be derived by examining the action of $\mathcal{T}^{(+)}$ and $\mathcal{T}^{(-)}$ on the basis states (5). A similar derivation for a different basis is described, e.g., in Refs. [21,22]. Let us note that it follows from the antisymmetry of the two-nucleon states and from the symmetry properties of the HO brackets that the contributions of $\mathcal{T}^{(-)}$ and $\mathcal{T}^{(+)}$ in Eq. (9) are identical.

The eigensystem of the operator \mathcal{T} , Eq. (8), consists of two subspaces. The first subspace has eigenstates with eigenvalue 3, which form totally antisymmetric physical states. The second subspace has eigenstates with eigenvalue 0, which form a not completely antisymmetric, unphysical subspace of states. We found these properties of \mathcal{T} by direct calculation using the relation (9). It is, however, a general result. The same structure of eigenstates was also obtained in Ref. [23] using a different basis. The eigenvalue structure follows from the fact that $\frac{1}{3}\mathcal{T}$ has the properties of a projection operator. It is possible to Hermitize the Hamiltonian (7) on the physical subspace, where it is quasi-Hermitian. The Hermitized Hamiltonian takes the form

$$\bar{H} = H_0 + \bar{\mathcal{T}}^{1/2} V(\vec{r}) \bar{\mathcal{T}}^{1/2}, \tag{10}$$

where $\bar{\mathcal{T}}$ operates on the physical subspace only.

The operator \mathcal{T} , Eq. (8), is diagonal in $N = 2n + l + 2\mathcal{N} + \mathcal{L}$. Note that any basis truncation other than one of the type $N \leq N_{\max}$ violates, in general, the Pauli principle and mixes physical and unphysical states. Here, N_{\max} characterizes the maximum of total allowed HO quanta in the model space and is an input parameter of the calculation. The truncation into totally allowed oscillator quanta $N \leq N_{\max}$, however, preserves the equivalence of the Hamiltonians (7) and (10) on the physical subspace.

B. Four-nucleon system

By relying on the results obtained for the three-nucleon system, as described in the previous subsection, we can extend the formalism to the four-nucleon system. We use the Hamiltonian (2) with $A=4$. By introducing the coordinate (and momentum) transformations

$$\vec{r} = \sqrt{\frac{1}{2}}(\vec{r}_1 - \vec{r}_2), \tag{11a}$$

$$\vec{z} = \sqrt{\frac{2}{3}}[\frac{1}{2}(\vec{r}_1 + \vec{r}_2) - \vec{r}_3], \tag{11b}$$

$$\vec{z} = \frac{\sqrt{3}}{2}[\frac{1}{3}(\vec{r}_1 + \vec{r}_2 + \vec{r}_3) - \vec{r}_4], \tag{11c}$$

we obtain the one-body part of the Hamiltonian (2) in the form

$$H_0 = \frac{\vec{p}^2}{2m} + \frac{1}{2}m\Omega^2\vec{r}^2 + \frac{\vec{q}^2}{2m} + \frac{1}{2}m\Omega^2\vec{y}^2 + \frac{\vec{o}^2}{2m} + \frac{1}{2}m\Omega^2\vec{z}^2, \tag{12}$$

with the center-of-mass term omitted.

A possible generalization of the Faddeev equation (6) for four identical particles can be written in the form

$$\bar{H}|\psi_{(123)4}\rangle = E|\psi_{(123)4}\rangle, \tag{13}$$

with

$$\begin{aligned}
\bar{H}|\psi_{(123)4}\rangle &\equiv H_0|\psi_{(123)4}\rangle + \frac{1}{2}(V_{12} + V_{13} + V_{23}) \\
&\times (|\psi_{(123)4}\rangle + |\psi_{(432)1}\rangle + |\psi_{(134)2}\rangle + |\psi_{(142)3}\rangle)
\end{aligned} \tag{14}$$

and

$$\begin{aligned}
& (|\psi_{(123)4}\rangle + |\psi_{(432)1}\rangle + |\psi_{(134)2}\rangle + |\psi_{(142)3}\rangle) \\
&= (1 - \mathcal{T}_{14} - \mathcal{T}_{24} - \mathcal{T}_{34})|\psi_{(123)4}\rangle \equiv \mathcal{T}_4|\psi_{(123)4}\rangle.
\end{aligned} \tag{15}$$

Here, $|\psi_{(123)4}\rangle$ is a four-fermion Faddeev amplitude completely antisymmetrized for particles 1, 2, and 3. There are three other equations that can be obtained from Eq. (13) by permuting particle 4 with particles 1, 2, and 3. Their sum then leads to the Schrödinger equation. We note that the present equations are different from the traditional Faddeev-Yakubovskii equations [7], which combine Faddeev amplitudes depending on two sets of relative coordinates. We are working with a complete orthonormal basis. It is, therefore, sufficient and convenient to use a single set of coordinates defined by the relations (11). Unlike the Faddeev amplitudes used typically in the Faddeev-Yakubovskii equations, the

amplitudes appearing in Eq. (13) are antisymmetrized with respect to the first three particles. Those amplitudes are obtained, as described below, in a straightforward manner with the help of our three-nucleon HO formalism introduced earlier. The present equations allow us to employ easily real three-body interactions or three-body effective interactions. The latter property makes them particularly useful for the present extension of shell-model calculations for four nucleons. At the same time, the use of Faddeev amplitudes antisymmetrized for particles 1, 2, and 3 allows us to reduce the dimension of the basis significantly.

We start the four-nucleon calculation using the basis

$$|N_1 i J_1 T_1, n_z l_z \mathcal{J}_4, J T\rangle, \quad (16)$$

with the three-fermion part given by the antisymmetrized eigenstates of \mathcal{T} , Eq. (8), corresponding to eigenvalue 3, e.g.,

$$|N_1 i J_1 T_1\rangle = \sum c_{nlsjt, \mathcal{N}\mathcal{L}\mathcal{J}_3}^{N_1 i J_1 T_1} |nlsjt, \mathcal{N}\mathcal{L}\mathcal{J}_3, J_1 T_1\rangle, \quad (17)$$

where $N_1 = 2n + l + 2\mathcal{N} + \mathcal{L}$ and i counts the eigenstates of \mathcal{T} with eigenvalue 3 for a given N_1 and J_1, T_1 . Further, n_z, l_z are the HO quantum numbers corresponding to the harmonic oscillator associated with the coordinate \vec{z} and the momentum \vec{o} and \mathcal{J}_4 is the angular momentum of the fourth particle relative to the center of mass of particles 1, 2, and 3.

As in the case of the three-particle transposition operators (9), a compact formula can be derived for the matrix elements of the four-particle transposition operators in the basis (16), e.g.,

$$\begin{aligned} & \langle N_{1L} i_L J_{1L} T_{1L}, n_{zL} l_{zL} \mathcal{J}_{4L}, J T | \mathcal{T}_{14} + \mathcal{T}_{24} + \mathcal{T}_{34} | N_{1R} i_R J_{1R} T_{1R}, n_{zR} l_{zR} \mathcal{J}_{4R}, J T \rangle \\ &= \delta_{N_L, N_R} \sum c_{n_L l_L s_L j_L t_L \mathcal{N}_L \mathcal{L}_L \mathcal{J}_{3L}}^{N_{1L} i_L J_{1L} T_{1L}} c_{n_R l_R s_R j_R t_R \mathcal{N}_R \mathcal{L}_R \mathcal{J}_{3R}}^{N_{1R} i_R J_{1R} T_{1R}} \hat{L}_{1L}^2 \hat{L}_{1R}^2 \hat{S}_{1L}^2 \hat{S}_{1R}^2 \hat{L}_2^2 \hat{L}_2^2 \hat{J}_L^2 \hat{J}_R^2 \hat{\mathcal{J}}_3 \hat{\mathcal{J}}_3 \hat{\mathcal{J}}_4 \hat{\mathcal{J}}_4 \hat{J}_{1L} \hat{J}_{1R} \hat{T}_{1L} \hat{T}_{1R} \\ & \times (-1)^{T_{1L} - T_{1R} + S_{1L} + S_{1R}} \begin{Bmatrix} \frac{1}{2} & s_R & S_{1R} \\ \frac{1}{2} & S_2 & S_{1L} \end{Bmatrix} \begin{Bmatrix} \frac{1}{2} & t_R & T_{1R} \\ \frac{1}{2} & T & T_{1L} \end{Bmatrix} \begin{Bmatrix} l_L & s_L & j_L \\ \mathcal{L}_L & \frac{1}{2} & \mathcal{J}_{3L} \\ L_{1L} & S_{1L} & J_{1L} \end{Bmatrix} \begin{Bmatrix} l_R & s_R & j_R \\ \mathcal{L}_R & \frac{1}{2} & \mathcal{J}_{3R} \\ L_{1R} & S_{1R} & J_{1R} \end{Bmatrix} \\ & \times \begin{Bmatrix} L_{1L} & S_{1L} & J_{1L} \\ l_{zL} & \frac{1}{2} & \mathcal{J}_{4L} \\ L_2 & S_2 & J \end{Bmatrix} \begin{Bmatrix} L_{1R} & S_{1R} & J_{1R} \\ l_{zR} & \frac{1}{2} & \mathcal{J}_{4R} \\ L_2 & S_2 & J \end{Bmatrix} \hat{L}'^2 (-1)^{L'} \begin{Bmatrix} l_R & L_2 & L' \\ l_{zR} & \mathcal{L}_R & L_{1R} \end{Bmatrix} \begin{Bmatrix} l_R & L_2 & L' \\ l_{zL} & l' & L_{1L} \end{Bmatrix} \left[\hat{S}_L \hat{S}_R \hat{t}_L \hat{t}_R \begin{Bmatrix} \frac{1}{2} & \frac{1}{2} & s_R \\ \frac{1}{2} & S_{1L} & s_L \end{Bmatrix} \right] \\ & \times \begin{Bmatrix} \frac{1}{2} & \frac{1}{2} & t_R \\ \frac{1}{2} & T_{1L} & t_L \end{Bmatrix} (-1)^{l_{zR} + L_{1L}} (-1)^{l_{zL}} \langle n' l' n_{zL} l_{zL} L' | n_{zR} l_{zR} \mathcal{N}_R \mathcal{L}_R L' \rangle_8 \langle n_L l_L \mathcal{N}_L \mathcal{L}_L L_{1L} | n' l' n_R l_R L_{1L} \rangle_3 \\ & + (-1)^{t_R - t_L + s_R - s_L + \mathcal{L}_R - l_L - \mathcal{L}_L} \langle n_{zL} l_{zL} n' l' L' | \mathcal{N}_R \mathcal{L}_R n_{zR} l_{zR} L' \rangle_8 \langle \mathcal{N}_L \mathcal{L}_L n_L l_L L_{1L} | n_R l_R n' l' L_{1L} \rangle_3 \\ & - \delta_{l_L, l_R} \delta_{s_L, s_R} \delta_{t_L, t_R} \delta_{\mathcal{N}_L, n'} \delta_{\mathcal{L}_L, l'} (-1)^{\mathcal{L}_R + l_{zR}} \langle n_{zL} l_{zL} \mathcal{N}_L \mathcal{L}_L L' | \mathcal{N}_R \mathcal{L}_R n_{zR} l_{zR} L' \rangle_8 \Big], \quad (18) \end{aligned}$$

where $N_X = 2n_X + l_X + 2\mathcal{N}_X + \mathcal{L}_X + 2n_{zX} + l_{zX}$, $X \equiv L$ or R , and, e.g., the expression $\langle n_{zL} l_{zL} \mathcal{N}_L \mathcal{L}_L L' | \mathcal{N}_R \mathcal{L}_R n_{zR} l_{zR} L' \rangle_8$ denotes a general HO bracket for two particles with mass ratio 8, as defined in Ref. [20]. Similarly, as in Eq. (9) the brackets for two particles with mass ratio 3 also appear in the relation (18). In the derivation of expression (18) we relied on the antisymmetry of the basis states with respect to particles 1, 2, and 3. The calculation was facilitated by application of the operators $-\mathcal{T}_{13}$ and $-\mathcal{T}_{23}$. The relation (18) appears to be nonsymmetric. However, its numerical evaluation leads to a symmetric matrix. It may also appear that the angular momentum sums in Eq. (18) can be summed up. In fact, it is possible to simplify the expression by introducing a $15j$ coefficient of the fifth kind as defined, e.g., in Ref. [24], but as such coefficients are seldomly used, we prefer to keep the summations in the explicit form. On the other hand, a significant simplification of expression (18) can be obtained, when the symmetry relations of different terms are exploited. First, it follows from the properties of the HO brackets and from the antisymmetry of the two-nucleon states that the contributions of \mathcal{T}_{14} and \mathcal{T}_{24} are identical. Second, using the fact that the states (16) are antisymmetrized for the particles 1, 2, and 3 it follows that all three permutation operators appearing in Eq. (18) give identical contributions to expression (18). The computation of \mathcal{T}_{34} is the simplest. In that case a partial summation of the angular momentum coefficients can be performed, yielding a compact expression

$$\begin{aligned}
& \langle N_{1L}i_L J_{1L} T_{1L}, n_{zL} l_{zL} \mathcal{J}_{4L}, JT | \mathcal{T}_{34} | N_{1R}i_R J_{1R} T_{1R}, n_{zR} l_{zR} \mathcal{J}_{4R}, JT \rangle \\
&= \delta_{N_L, N_R} \sum c_{nlsjt N_L \mathcal{L}_L \mathcal{J}_{3L}}^{N_{1L} i_L J_{1L} T_{1L}} c_{nlsjt N_R \mathcal{L}_R \mathcal{J}_{3R}}^{N_{1R} i_R J_{1R} T_{1R}} \hat{\mathcal{J}}_{3L} \hat{\mathcal{J}}_{3R} \hat{\mathcal{J}}_{4L} \hat{\mathcal{J}}_{4R} \hat{J}_{1L} \hat{J}_{1R} \hat{T}_{1L} \hat{T}_{1R} (-1)^{T_{1L} + T_{1R} + \mathcal{J}_{3L} + \mathcal{J}_{3R}} \begin{Bmatrix} \frac{1}{2} & t & T_{1R} \\ \frac{1}{2} & T & T_{1L} \end{Bmatrix} \\
&\times \hat{K}^2 \begin{Bmatrix} j & \mathcal{J}_{3L} & J_{1L} \\ \mathcal{J}_{3R} & K & \mathcal{J}_{4L} \\ J_{1R} & \mathcal{J}_{4R} & J \end{Bmatrix} \begin{Bmatrix} \mathcal{L}_L & l_{zR} & K \\ \mathcal{J}_{4R} & \mathcal{J}_{3L} & \frac{1}{2} \end{Bmatrix} \begin{Bmatrix} \mathcal{L}_R & l_{zL} & K \\ \mathcal{J}_{4L} & \mathcal{J}_{3R} & \frac{1}{2} \end{Bmatrix} \begin{Bmatrix} l_{zL} & \mathcal{L}_R & K \\ l_{zR} & \mathcal{L}_L & L' \end{Bmatrix} \\
&\times \hat{L}'^2 (-1)^{\mathcal{L}_R + l_{zL} + L'} \langle n_{zL} l_{zL} \mathcal{N}_L \mathcal{L}_L L' | \mathcal{N}_R \mathcal{L}_R n_{zR} l_{zR} L' \rangle_8. \tag{19}
\end{aligned}$$

Thus, by multiplying expression (19) by 3 we obtain the same matrix element as from Eq. (18). We note that a generalization of the evaluation of the permutation operator matrix element (19) to a system more complex than the presently studied $A=4$ system is straightforward. Its simplicity suggests that the present formalism can be extended to systems with $A>4$.

Similarly, as for the operator \mathcal{T} , Eq. (8), eigenstates of the operator \mathcal{T}_4 defined by the relation (15) can be subdivided into two subspaces. A physical subspace is spanned by totally antisymmetric states, in this case corresponding to eigenvalue 4, and a spurious subspace is spanned by eigenvectors corresponding to eigenvalue 0. It is possible to symmetrize the Hamiltonian \tilde{H} appearing in Eq. (13) on the physical subspace. The symmetrized Hamiltonian then takes the form

$$\tilde{H} = H_0 + \bar{\mathcal{T}}_4^{1/2} \frac{1}{2} (V_{12} + V_{13} + V_{23}) \bar{\mathcal{T}}_4^{1/2}, \tag{20}$$

where $\bar{\mathcal{T}}_4$ operates only on the physical subspace. In our calculations, described later, we diagonalize the symmetrized Hamiltonian (20) in the physical basis formed by the eigenstates of $\bar{\mathcal{T}}_4$.

The operator $\bar{\mathcal{T}}_4$, Eq. (15) is diagonal in $N=2n+l+2\mathcal{N}+2n_z+l_z$. A basis truncation defined by a restriction on the totally allowed oscillator quanta $N \leq N_{\max}$ preserves the equivalence of the Hamiltonians (14) and (20) on the physical subspace.

C. Effective interactions

From solving two-nucleon systems in a HO well, interacting by soft-core potentials, one learns that excitations up to about $300\hbar\Omega$ ($N_{\max}=300$) are required to get almost exact solutions. We anticipate, therefore, that at least the same number of excitations should be allowed to solve the many-nucleon system. The Faddeev formulation has the obvious advantage compared with the traditional shell-model approach that the center-of-mass coordinate is explicitly removed. Even then, it is not feasible to solve the eigenvalue problem either for Eqs. (10) or (20) in such a large space. On the other hand, shell-model calculations are always performed by employing effective interactions tailored to a specific model space. In practice, these effective interactions can never be calculated exactly, because, in general, an A -body effective interaction is required for an A -nucleon system. We

may, however, take advantage of the present approach to perform shell-model calculations in significantly larger model spaces than are possible in a conventional shell-model approach. At the same time we can investigate convergence properties of effective interactions. If convergence is achieved, we should obtain the exact solution, since by construction the effective interactions that we employ satisfy the condition $V_{\text{eff}} \rightarrow V$ for $N_{\max} \rightarrow \infty$.

Usually, the effective interaction is approximated by a two-body effective interaction determined from a two-nucleon system. In the present calculations we replace matrix elements of the potential $V(\vec{r})$ by matrix elements of an effective two-body interaction, derived in a straightforward manner for each relative-coordinate partial channel. The relevant two-nucleon Hamiltonian is then

$$H_2 \equiv H_{02} + V = \frac{\vec{p}^2}{2m} + \frac{1}{2} m \Omega^2 \vec{r}^2 + V_N(\sqrt{2}\vec{r}) - \frac{m\Omega^2}{A} \vec{r}^2, \tag{21}$$

which can be solved as a differential equation or, alternatively, can be diagonalized in a sufficiently large harmonic oscillator basis. For a four-nucleon system we set $A=4$ in Eq. (21), which implies that we are dealing with a bound-state problem.

To construct the two-body effective interaction we employ the Lee-Suzuki [25] similarity transformation method, which gives an effective interaction in the form $PV_{\text{eff}}P = PVP + PVQ\omega P$, with ω the transformation operator satisfying $\omega = Q\omega P$, and P and $Q = 1 - P$, the projectors on the model and the complementary spaces, respectively. Our calculations start with exact solutions of the Hamiltonian (21) and, consequently, we construct the operator ω and, then, the effective interaction directly from these solutions. Let us denote the relative-coordinate two-nucleon HO states, which form the model space, as $|\alpha_P\rangle$, and those which belong to the Q space, as $|\alpha_Q\rangle$. Then the Q -space components of the eigenvector $|k\rangle$ of the Hamiltonian (21) can be expressed as a combination of the P -space components with the help of the operator ω :

$$\langle \alpha_Q | k \rangle = \sum_{\alpha_P} \langle \alpha_Q | \omega | \alpha_P \rangle \langle \alpha_P | k \rangle. \tag{22}$$

If the dimension of the model space is d_P , we may choose a set \mathcal{K} of d_P eigenvectors, for which the relation (22) will be

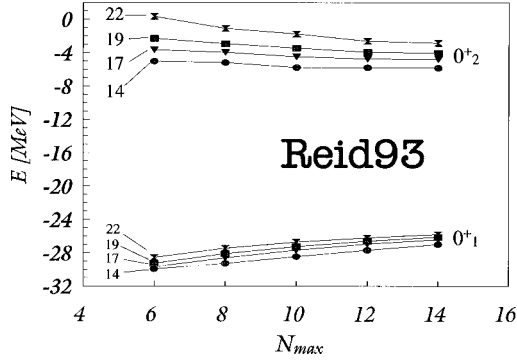


FIG. 1. The dependence of the ground-state and the first-excited 0^+0 state energies, in MeV, on the maximal number of HO excitations allowed in the model space. The two-body effective interaction utilized was derived from the Reid93 NN potential. Results for $\hbar\Omega = 14, 17, 19,$ and 22 MeV are presented.

satisfied. Under the condition that the $d_p \times d_p$ matrix $\langle \alpha_p | k \rangle$ for $|k\rangle \in \mathcal{K}$ is invertible, the operator ω can be determined from Eq. (22). In the present application we select the lowest states obtained in each channel. Their number is given by the number of basis states satisfying $2n+l \leq N_{\max}$. Once the operator ω is determined, the effective Hamiltonian can be constructed as follows:

$$\langle \gamma_P | H_{2\text{eff}} | \alpha_P \rangle = \sum_{k \in \mathcal{K}} \left[\langle \gamma_P | k \rangle E_k \langle k | \alpha_P \rangle + \sum_{\alpha_Q} \langle \gamma_P | k \rangle E_k \langle k | \alpha_Q \rangle \langle \alpha_Q | \omega | \alpha_P \rangle \right]. \quad (23)$$

It should be noted that $P|k\rangle = \sum_{\alpha_p} |\alpha_p\rangle \langle \alpha_p | k \rangle$ for $|k\rangle \in \mathcal{K}$ is a right eigenvector of Eq. (23) with the eigenvalue E_k .

This Hamiltonian, when diagonalized in a model-space basis, reproduces exactly the set \mathcal{K} of d_p eigenvalues E_k . Note that the effective Hamiltonian is, in general, quasi-Hermitian. It can be Hermitized by a similarity transformation determined from the metric operator $P(1 + \omega^\dagger \omega)P$. The Hermitian Hamiltonian is then given by [26]

$$\bar{H}_{2\text{eff}} = [P(1 + \omega^\dagger \omega)P]^{1/2} H_{2\text{eff}} [P(1 + \omega^\dagger \omega)P]^{-1/2}. \quad (24)$$

Finally, the two-body effective interaction used in the present calculations is determined from the two-nucleon effective Hamiltonian (24) as $V_{2\text{eff}} = \bar{H}_{2\text{eff}} - H_{02}$. We note that the interaction $V_{12} + V_{13} + V_{23}$ in Eq. (20) is then replaced by $T^{1/2} V_{2\text{eff}} T^{1/2}$, which is evaluated in a straightforward way in the basis (16).

As pointed out before, the structure of the Hamiltonian (20) allows us to employ easily three-body effective interactions in addition to the above-discussed two-body effective interactions. We can replace $V_{12} + V_{13} + V_{23}$ in Eq. (20) by $V_{3\text{eff}}$, which can be derived from the three-nucleon solutions in a similar manner as the two-body effective interaction is derived from the two-nucleon solutions. To find $V_{3\text{eff}}$ we solve the three-nucleon system described by the Hamiltonian (10) with $V(\vec{r}) = V_N(\sqrt{2}\vec{r}) - (1/A)m\Omega^2\vec{r}^2$. As $A=4$ we are dealing with a bound three-nucleon problem. It can be solved in a three-nucleon model space characterized by $N_{3\text{max}} \approx 30$

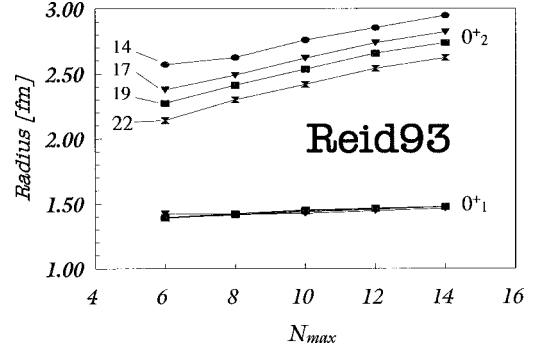


FIG. 2. The dependence of the point-nucleon rms radius of the ground state and the first-excited 0^+0 state, in fm, on the maximal number of HO excitations allowed in the model space. The two-body effective interaction utilized was derived from the Reid93 NN potential. Results for $\hbar\Omega = 14, 17, 19,$ and 22 MeV are presented.

[13]. First, we compute the two-body effective interaction appropriate for the model space defined by $N_{3\text{max}}$, as discussed earlier in this subsection. Then the three-nucleon system is solved in the same space. Afterwards we construct the three-body effective interaction for a model space defined by $N_{\max} < N_{3\text{max}}$. In the present paper we use model spaces up to $N_{\max} = 14$. The effective interaction is constructed exactly, as described above, using Eqs. (22), (23), and (24) with $H_{2\text{eff}}$ replaced by $H_{3\text{eff}}$. The energies E_k and the states $|k\rangle$ correspond to the three-nucleon system eigenstates, however, and the states $|\alpha_P\rangle$ and $|\alpha_Q\rangle$ are three-nucleon basis states (17) with the model-space condition $N_1 \equiv 2n+l+2\mathcal{N}+\mathcal{L} \leq N_{\max}$ and the Q -space condition $N_{\max} < N_1 \leq N_{3\text{max}}$. The three-body effective interaction is computed for different three-nucleon channels characterized by J_1 , T_1 , and parity and is obtained from the Hermitized effective Hamiltonian as $V_{3\text{eff}} = \bar{H}_{3\text{eff}} - H_0$, where H_0 is given by Eq. (4). The interaction $V_{3\text{eff}}$ then replaces $V_{12} + V_{13} + V_{23}$ in Eq. (20). We note that by construction in the limit $N_{\max} \rightarrow N_{3\text{max}}$ the three-body effective interaction approaches the two-body effective interaction $V_{3\text{eff}} \rightarrow T^{1/2} V_{2\text{eff}} T^{1/2}$ and with $N_{\max} \rightarrow \infty$ the effective interaction approaches the bare interaction $V_{2\text{eff}} \rightarrow V$.

III. APPLICATION TO ^4He

In the present paper we use the Reid93 NN potential [27] and the Argonne V8' NN potential, introduced in Ref. [9]. We work in the isospin formalism; the charge-invariant potential $V_N = \frac{1}{3}V_{pp} + \frac{1}{3}V_{nn} + \frac{1}{3}V_{np}$ is used for each $T=1$ wave in the calculations with the Reid93 potential. The Coulomb potential is added to V_{pp} in this case. On the other hand, the calculations with the Argonne V8' potential, which is isopin invariant, do not include the Coulomb potential.

Our calculation progresses in several steps. The model space is characterized by the condition $N \leq N_{\max}$, $N = 2n + l + 2\mathcal{N} + \mathcal{L} + 2n_z + l_z$. First, the three-nucleon antisymmetrized basis is constructed by diagonalizing \mathcal{T} , Eq. (8), in the basis (5) for all $N_1 \equiv 2n+l+2\mathcal{N}+\mathcal{L} \leq N_{\max}$ and all J_1, T_1 . Then the four-nucleon antisymmetrized basis is calculated by diagonalizing \mathcal{T}_4 , Eq. (15), in the basis (16) for $N = N_1 + 2n_z + l_z \leq N_{\max}$ with N even for positive-parity states and N odd for negative-parity states. We present results for $J=0$ and $T=0$ only, but for both parities. We note that the four-

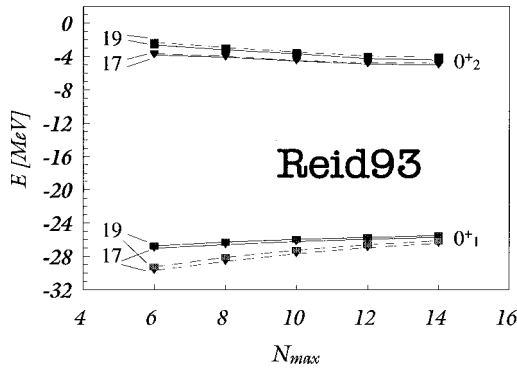


FIG. 3. The dependence of the ground-state and the first-excited 0^+_0 state energies, in MeV, on the maximal number of HO excitations allowed in the model space. Results obtained using the two-body (dashed line) and three-body (solid line) effective interaction derived from the Reid93 NN potential are compared. Harmonic-oscillator energies of $\hbar\Omega = 17$ and 19 MeV were used.

nucleon basis computation is independent of Ω and is done only once. The next step is the effective interaction calculation. The two-body effective interaction is derived from Eqs. (22)–(24). The condition for the relative-coordinate two-body effective-interaction model space is then $2n+l \leq N_{max}$. When solving the two-nucleon relative-coordinate Hamiltonian (21) in the full space, we truncate the HO basis by keeping the states typically up to $n = 152$. The two-body effective interaction is constructed for all partial-wave channels up to $j = 6$. The resulting effective interaction is finally used as input for the four-nucleon calculation, where the Hamiltonian (20) is diagonalized. Instead of a two-body effective interaction, we may use a three-body effective interaction, as discussed in the previous section. The three-body effective is computed only for the most important three-nucleon channels $J_1 T_1$. In particular, we evaluated the three-body effective interaction for $J_1 = 1/2, 3/2$, $T_1 = 1/2$, and for both positive and negative parity. For the channels with higher J_1 the two-body effective interaction corresponding to N_{max} is used instead. For the parameter N_{3max} characterizing the three-nucleon full space, we used $N_{3max} = 28$ for J_1

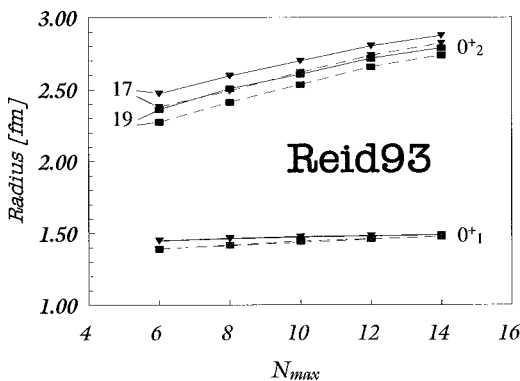


FIG. 4. The dependence of the point-nucleon rms radius of the ground state and the first-excited 0^+_0 state, in fm, on the maximal number of HO excitations allowed in the model space. Results obtained using the two-body (dashed line) and three-body (solid line) effective interaction derived from the Reid93 NN potential are compared. Harmonic-oscillator energies of $\hbar\Omega = 17$ and 19 MeV were used.

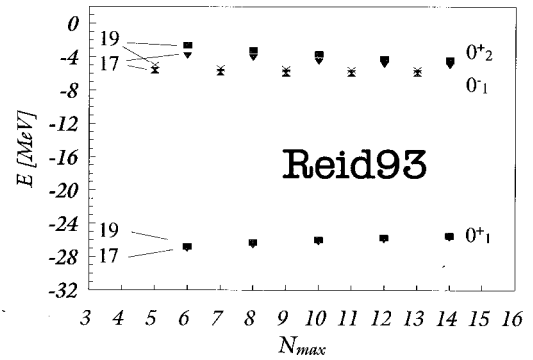


FIG. 5. The dependence of the ground state, the first-excited 0^+_0 state, and the first-excited 0^-_0 state energies, in MeV, on the maximal number of HO excitations allowed in the model space. For the positive-parity states the results were obtained using the three-body effective interaction derived from the Reid93 NN potential. Energies of the 0^-_0 state were calculated using a two-body effective interaction derived from the Reid93 NN potential. Harmonic-oscillator energies of $\hbar\Omega = 17$ and 19 MeV were used.

$= 1/2$ and $N_{3max} = 24$ for $J_1 = 3/2$. We also performed calculations with the inclusion of the three-body effective interaction for $J_1 = 5/2$ and found it to have little effect.

Let us remark that the present method for solving the four-nucleon shell-model problem is fully equivalent to the standard shell-model approach. In particular, it is straightforward to transform the relative-coordinate two-body effective interaction used in the present calculations to the two-particle basis used for the shell-model input by the standard transformation [28]. We used the transformed interactions for the model spaces up to an $8\hbar\Omega$ space to test our results. The shell-model diagonalization was then performed by employing the many-fermion-dynamics shell-model code [29], which can be utilized for calculations with model spaces comprising up to 9 major HO shells, i.e., $N_{max} = 8$ for ${}^4\text{He}$. We obtained the same results from both the Faddeev-like calculation and the standard shell-model calculation. The Faddeev-like calculation has, obviously, much smaller di-

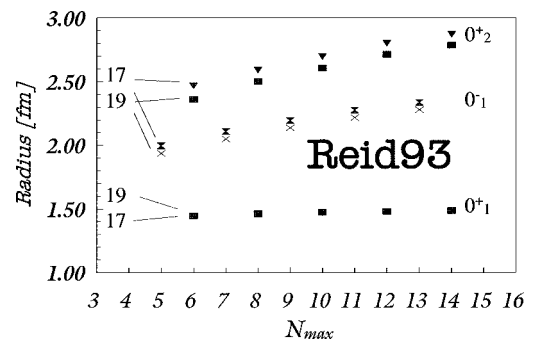


FIG. 6. The dependence of the point-nucleon rms radius of the ground state, the first-excited 0^+_0 state, and the first-excited 0^-_0 state, in fm, on the maximal number of HO excitations allowed in the model space. For the positive-parity states the results were obtained using the three-body effective interaction derived from the Reid93 NN potential. Energies of the 0^-_0 state were calculated using a two-body effective interaction derived from the Reid93 NN potential. Harmonic-oscillator energies of $\hbar\Omega = 17$ and 19 MeV were used.

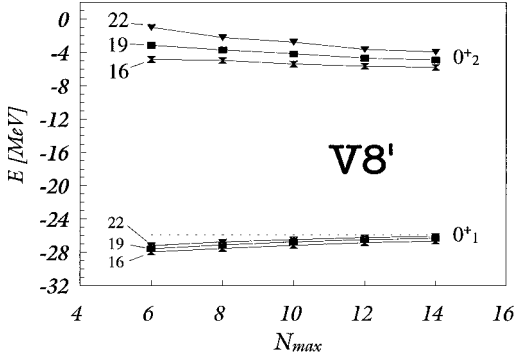


FIG. 7. The dependence of the ground-state and the first-excited 0^+0 state energies, in MeV, on the maximal number of HO excitations allowed in the model space. The three-body effective interaction derived from the Argonne V8' NN potential was used. Results for $\hbar\Omega = 16, 19,$ and 22 MeV are presented. The dotted line represents the result, -25.92 MeV, of the GFMC calculation [34].

mension and can be extended to larger model spaces. We also note that we applied the discussed formalism to four-electron system in a related study recently [30]. Our results compared well with those obtained by the stochastic variational method [31].

A. Energies and point-nucleon rms radii

Our results for the ground-state and excited-state energies and point-nucleon rms radii are presented in Figs. 1–9, where the dependences on the model-space size and the HO energy are shown. A summary of the largest model-space ($N_{\max} = 14$ for the positive-parity states and $N_{\max} = 13$ for the negative-parity states) results is given in Table II. Let us mention an unusual feature of the present calculations, namely, the convergence from below for the ground-state energy. It is caused by the asymmetric treatment of the HO terms that are added and subtracted to the Hamiltonian in the process of evaluating the effective interaction. Our effective interaction is computed for a two- or three-nucleon system bound in a HO potential. Therefore, artificial binding from this potential is included in the effective interaction and the

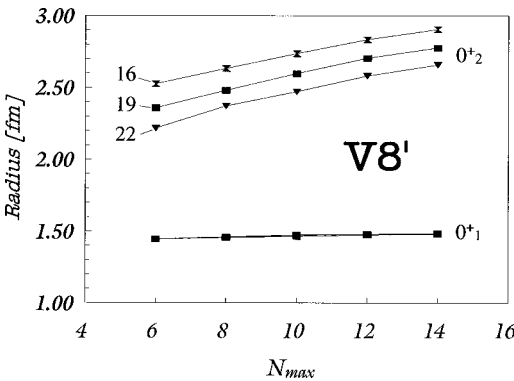


FIG. 8. The dependence of the point-nucleon rms radius of the ground state and the first-excited 0^+0 state, in fm, on the maximal number of HO excitations allowed in the model space. The three-body effective interaction derived from the Argonne V8' NN potential was used. Results for $\hbar\Omega = 16, 19,$ and 22 MeV are presented.

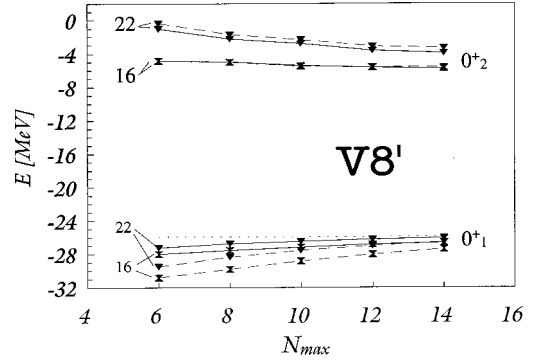


FIG. 9. The dependence of the ground-state and the first-excited 0^+0 state energies, in MeV, on the maximal number of HO excitations allowed in the model space. Results obtained using the two-body (dashed line) and three-body (solid line) effective interaction derived from the Argonne V8' NN potential are compared. Harmonic-oscillator energies of $\hbar\Omega = 16$ and 22 MeV were used. The dotted line represents the result, -25.92 MeV, of the GFMC calculation [34].

four-body effects coming from the entire four-nucleon calculation may not completely compensate for this spurious binding in a particular model space. We note that this type of overbinding in the no-core shell-model calculations was noticed in previous studies [32,33,12]. This effect decreases as the model-space size increases, as is demonstrated in our earlier three-nucleon shell-model calculations [13].

In Fig. 1 we present the calculated dependence of the ground-state energy and the first-excited 0^+0 state energy on the model-space size, characterized by N_{\max} . The two-body effective interaction employed was derived from the Reid93 NN potential. Results for $\hbar\Omega = 14, 17, 19, 22$ MeV are shown. The corresponding dependence of the point-nucleon rms radius is presented in Fig. 2. A slow convergence with the increasing model-space size can be observed for energies with a significantly faster rate for the ground state compared to the first-excited 0^+0 state. Also, a much stronger dependence of the excited state on the HO energy $\hbar\Omega$ is apparent. The results of the point-nucleon rms-radius calculation demonstrate even more the differences between the ground state and the first-excited 0^+0 state. While the ground-state radius has almost converged and shows little $\hbar\Omega$ dependence, the first-excited 0^+0 state displays a strong dependence of its energy on $\hbar\Omega$ and a steady increase of its radius with increasing model-space size.

Let us remark that in our approach we obtain the ground state as well as the excited states by diagonalizing the Hamiltonian. This implies that the excited states are expanded in

TABLE I. Absolute value of the ground-state energy differences obtained in the calculations with HO energies of $\hbar\Omega = 16$ MeV and $\hbar\Omega = 22$ MeV with the two-body (second row) and the three-body (third row) effective interactions in different model spaces. The effective interactions were derived from the Argonne V8' NN potential. The corresponding energy dependence is shown in Fig. 9.

N_{\max}	6	8	10	12	14
$ \Delta E_{2 \text{ eff}} $	1.311	1.466	1.265	1.037	0.834
$ \Delta E_{3 \text{ eff}} $	0.778	0.782	0.676	0.601	0.550

the same harmonic-oscillator basis used for the ground state. While such an approach has technical advantages, it might not be physically sound. Cautious interpretation of the excited-state results is, therefore, necessary. The significantly different convergence rate of the ground state and of the first-excited 0^+0 state manifests the different nature of the two states. Let us note that if the model-space size were increased up to the point at which total convergence of the excited state was achieved, our procedure would yield isolated three- and one-body clusters with an infinite rms radius and a total energy of the three-nucleon system. It is possible, though, that we could observe a metastability prior to the onset of the cluster separation, as the resonance is sharp and low lying. The present model-space sizes, however, are not yet sufficient to arrive at that point. That we have not reached this point can be seen from the lack of convergence and, in particular, from the rather small rms radius, which shows a significant increase with N_{\max} and a strong dependence on Ω .

The importance of the three-body effective interaction can be judged from the results shown in Fig. 3. The ground-state and excited 0^+0 state energies obtained in a calculation that employs the three-body effective interaction is compared to a calculation performed by using only the two-body effective interaction. Results for two different values of the HO energy, $\hbar\Omega = 17$ and 19 MeV, are presented. The dashed lines connect the two-body effective interaction calculation results that are identical to those in Fig. 1 that correspond to HO energies of $\hbar\Omega = 17$ and 19 MeV. The solid lines connect the results obtained in calculations with the three-body effective interaction. It is apparent that the three-body effective interaction improves the convergence considerably. It is especially true for the ground state. The difference between the $N_{\max} = 6$ and $N_{\max} = 14$ energies is significantly smaller in the calculation that employs the three-body effective interaction. It can also be seen that the two-body effective interaction results approach the three-body effective interaction results in the largest spaces used in our calculations. In addition, the dependence on the HO energy decreases in the three-body effective interaction calculation compared to the two-body effective interaction calculation. This holds for both the ground state and the first-excited 0^+0 state. However, the inclusion of the three-body effective interaction clearly has a larger overall impact on the ground-state results.

The influence of the three-body effective interaction on the point-nucleon rms radius is depicted in Fig. 4. Again we observe a better stability of the radii computed using the three-body effective interaction. In particular, the ground-state point-nucleon rms radius shows convergence in both the model-space-size dependence and the HO-frequency dependence. On the other hand, the three-body effective interaction does not improve the convergence of the excited state in any significant way in the model spaces that we employed.

In Fig. 5 we show the calculated energies of the first 0^-0 state obtained using two-body effective interactions in model spaces up to $N_{\max} = 13$. For a comparison, the results for the ground state and the first-excited 0^+0 state from Fig. 3 are also presented. It is interesting to note that the 0^-0 state shows a better convergence and stability with respect to the N_{\max} change as well as a weaker dependence on $\hbar\Omega$ than the

first-excited 0^+0 state. This observation is confirmed also in the point-nucleon rms radius calculation as can be seen in Fig. 6. In the experiment, the 0^-0 excitation energy, 21.01 MeV, is higher than the excitation energy of the first 0^+0 state, 20.21 MeV. Though in our calculations their positions are reversed, it is visible from Fig. 5 that the extrapolation to larger N_{\max} leads to correct ordering of the two states. A possible interpretation of this observation is that the excited 0^+0 state is associated with a radial excitation and, thus, it is more sensitive to the HO basis used in our calculations.

The energy and radius results, obtained using the Argonne V8' NN potential, are presented in Figs. 7 and 8, respectively. The three-body effective interaction was used in calculating these results, for three different HO energies, $\hbar\Omega = 16, 19,$ and 22 MeV. The dotted line represents the value -25.92 MeV obtained for the ground state, using the GFMC [34]. Similarly, as in the calculations with the Reid93 NN potential, we get the best convergence for the ground state for the highest value of $\hbar\Omega$, while for the excited state the best results are obtained for the lowest $\hbar\Omega$. The same discussion, given earlier, for the excited-state convergence using the Reid93 NN potential, is also valid for the calculations using the V8' NN potential. The energy convergence is very slow and there is no sign of convergence of the point-nucleon rms radius of the excited 0^+0 state. A significant dependence on $\hbar\Omega$ prevails for all the model spaces studied. On the other hand, the ground-state energy shows good convergence and approaches the GFMC result, in particular for the $\hbar\Omega = 22$ MeV calculation. The ground-state point-nucleon rms radius is almost $\hbar\Omega$ independent and converged. It agrees with the GFMC value of 1.485 fm.

We note that results on the first-excited 0^+0 state obtained using the resonating group method were reported in Ref. [17]. The Bonn potential employed in that work gives very similar results for the ground state as those obtained using the Argonne V8'. It is, therefore, reasonable to make a comparison for the excited-state results. The first-excited 0^+0 state energy reported in Ref. [17] was -6.42 MeV, which is about 10% below our result of $N_{\max} = 14$ and $\hbar\Omega = 16$ MeV calculation. The reported rms radius, 3.02 fm, is slightly above our calculation.

In order to further compare the convergence and the Ω dependence of the results obtained with two- and three-body effective interactions, we present a similar calculation as that of Fig. 3, obtained using the Argonne V8' NN potential and a larger Ω difference, in Fig. 9. The solid lines correspond to the three-body effective interaction calculations, also shown in Fig. 7, while the dashed lines connect the two-body effective interaction results. Two HO energies of $\hbar\Omega = 16$ and 22 MeV were used. The dotted line represents the GFMC result. Again we observe a better stability of the three-body effective-interaction results with respect to the model-space size changes, a smaller Ω dependence, and a faster convergence, in particular for the ground state. In Table I we show the absolute value of the ground-state energy differences obtained in the calculations with HO energies of $\hbar\Omega = 16$ MeV and $\hbar\Omega = 22$ MeV for both the two-body and the three-body effective-interaction calculations in different model spaces. We can see that the differences obtained with the three-body effective interaction are almost 2 times smaller in model spaces with $N_{\max} = 6-10$. The differences decrease with the

TABLE II. Results for the ground-state and excited-state energies and point-nucleon rms radii, as well as the excitation energies (E_x), obtained in the largest model spaces used in the present study, $N_{\max} = 14$ (13) for the positive- (negative-) parity states, respectively, are presented. All the states have isospin $T=0$. The positive-parity-state calculations were performed using the three-body effective interaction. Results for different HO energies are given in separate columns. The GFMC ground-state results [34] are shown for comparison.

Argonne V8' NN potential					
State	Variable	$\hbar\Omega = 16$ MeV	$\hbar\Omega = 19$ MeV	$\hbar\Omega = 22$ MeV	GFMC
0_1^+	E [MeV]	-26.62	-26.30	-26.07	-25.92(8)
	$\sqrt{\langle r^2 \rangle}$ [fm]	1.481	1.485	1.485	1.485(10)
0_2^+	E [MeV]	-5.77	-4.89	-3.93	
	E_x [MeV]	20.86	21.42	22.14	
	$\sqrt{\langle r^2 \rangle}$ [fm]	2.906	2.777	2.658	
0_1^-	E [MeV]	-6.70	-6.17	-5.59	
	E_x [MeV]	19.93	20.14	20.48	
	$\sqrt{\langle r^2 \rangle}$ [fm]	2.349	2.263	2.186	
Reid93 NN potential					
State	Variable	$\hbar\Omega = 17$ MeV	$\hbar\Omega = 19$ MeV		
0_1^+	E [MeV]	-25.69	-25.47		
	$\sqrt{\langle r^2 \rangle}$ [fm]	1.487	1.489		
0_2^+	E [MeV]	-5.00	-4.39		
	E_x [MeV]	20.69	21.08		
	$\sqrt{\langle r^2 \rangle}$ [fm]	2.873	2.787		
0_1^-	E [MeV]	-5.91	-5.54		
	E_x [MeV]	19.78	19.93		
	$\sqrt{\langle r^2 \rangle}$ [fm]	2.339	2.281		

enlargement of the model space for $N_{\max} \geq 8$. We note that by construction the present two- and three-body effective-interaction calculations would become identical for $N_{\max} = 28$.

In Table II we present a summary of our results obtained in the largest model spaces used in the present study, e.g., $N_{\max} = 14$ for the positive-parity states and $N_{\max} = 13$ for the negative-parity states. The positive-parity state results were obtained using the three-body effective interaction. For the Argonne V8' NN potential calculations we also include the GFMC ground-state results [34] for a comparison. We note that the Faddeev-Yakubovski equation solution gives -25.03 MeV [8] for the Nijmegen NN potential [35], which gives comparable results to the Reid93 NN potential for the three-nucleon problem. The experimental binding energy of ^4He is 28.296 MeV. The discrepancy between the experimental and calculated values is usually attributed to the real three-nucleon forces that were not taken into account either in our calculation or in the other calculations, which we discussed. We note that the difference in the binding energies obtained using the V8' and the Reid93 NN potentials is mainly due to the Coulomb interaction included in an isospin-invariant manner only in the calculations with the Reid93 NN potential.

B. Charge form factors

A sensitive test of the wave functions obtained in our calculations is the evaluation of charge form factors. Using the formalism of Ref. [36], we calculated the charge EM and strangeness form factors in the impulse approximation. The one-body contribution to the charge operator is given by Eq. (15) in Ref. [36], e.g.,

$$\hat{M}_{00}^{(a)}(q)^{[1]} = \frac{1}{2\sqrt{\pi}} \sum_{k=1}^A \left\{ \frac{G_E^{(a)}(\tau)}{\sqrt{1+\tau}} j_0(qr_k) + [G_E^{(a)}(\tau) - 2G_M^{(a)}(\tau)] 2\tau \frac{j_1(qr_k)}{qr_k} \boldsymbol{\sigma}_k \cdot \mathbf{L}_k \right\}, \quad (25)$$

where $\tau = q^2/4m_N^2$, \mathbf{L}_k is the k th nucleon orbital momentum, and $G_E^{(a)}(\tau)$ and $G_M^{(a)}(\tau)$ are the one-body electric and magnetic form factors, respectively. The superscript (a) refers to ($T=0$) for the isoscalar EM form factor or to (s) for the strangeness form factor. We use the parametrization of the one-body form factors as discussed in Ref. [36]:

$$G_E^{(p)}(\tau) = G_V^D(\tau), \quad (26a)$$

$$G_M^{(p)}(\tau) = \mu_p G_V^D(\tau), \quad (26b)$$

$$G_E^{(n)}(\tau) = -\mu_n \tau G_V^D(\tau) \xi_n(\tau), \quad (26c)$$

$$G_M^{(n)}(\tau) = \mu_n G_V^D(\tau), \quad (26d)$$

$$G_E^{(s)}(\tau) = \rho_s \tau G_V^D(\tau) \xi_s(\tau), \quad (26e)$$

$$G_M^{(s)}(\tau) = \mu_s G_V^D(\tau), \quad (26f)$$

with

$$G_V^D(\tau) = (1 + \lambda_V^D \tau)^{-2}, \quad (27a)$$

$$\xi_n = (1 + \lambda_n \tau)^{-1}, \quad (27b)$$

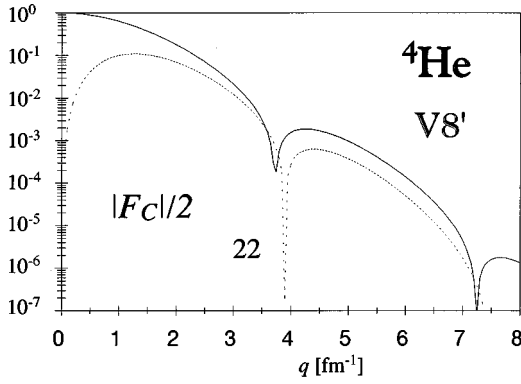


FIG. 10. The elastic EM charge form factor (solid line) and the EM charge form factor corresponding to the transition to the first-excited 0^+0 state (dotted line) calculated in the impulse approximation using the three-body effective interaction derived from the Argonne V8' NN potential in the $N_{\max}=14$ model space and $\hbar\Omega=22$ MeV.

$$\xi_s = (1 + \lambda_E^{(s)} \tau)^{-1}. \quad (27c)$$

The isoscalar EM form factor is given by $G_{E,M}^{(T=0)} = \frac{1}{2}[G_{E,M}^{(p)} + G_{E,M}^{(n)}]$, and for the parameters appearing in Eqs. (26) and (27), one has numerically $\mu_p = 2.79$, $\mu_n = -1.91$, $\lambda_V^D = 4.97$, and $\lambda_n = 5.6$. Following Ref. [36], we also set the strangeness radius $\rho_s = -2.0$ and $\lambda_E^{(s)} = \lambda_n$. Limits on these parameters are to be determined in the experiments at the Thomas Jefferson Accelerator Facility (TJNAF). The first strangeness magnetic-moment measurement was reported recently [37] and an experimental value $\mu_s = +0.23$, obtained with a large error. We use this value in our calculations.

Our charge form factor calculations are presented in Figs. 10–13. The charge form factors given in the figures were calculated using the one-body operator (25) as $F_C^{(a)}(q) = 2\sqrt{\pi}\langle f, 0^+0 | \hat{M}_{00}^{(a)}(q) | i, 0^+0 \rangle$. We show only results obtained with the Argonne V8' NN potential; the Reid93 NN potential gives almost identical results for the charge form factors, when the same HO energy $\hbar\Omega$ is employed. Our calculated elastic EM charge form factor is given in Fig. 10

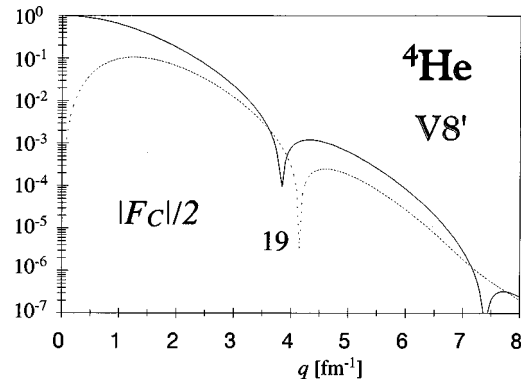


FIG. 11. The elastic EM charge form factor (solid line) and the EM charge form factor corresponding to the transition to the first-excited 0^+0 state (dotted line) calculated in the impulse approximation using the three-body effective interaction derived from the Argonne V8' NN potential in the $N_{\max}=14$ model space and $\hbar\Omega=19$ MeV.

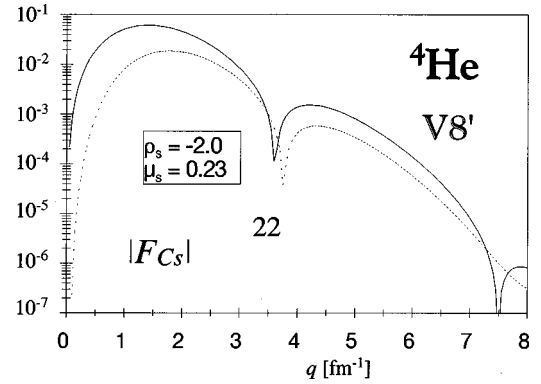


FIG. 12. The elastic strangeness charge form factor (solid line) and the strangeness charge form factor corresponding to the transition to the first-excited 0^+0 state (dotted line) calculated in the impulse approximation using the three-body effective interaction derived from the Argonne V8' NN potential in the $N_{\max}=14$ model space and $\hbar\Omega=22$ MeV. Values of the strangeness radius $\rho_s = -2.0$ and the strangeness magnetic moment $\mu_s = 0.23$ were employed.

together with the inelastic EM charge form factor corresponding to the transition to the first-excited 0^+0 state. These results were obtained using the HO energy $\hbar\Omega=22$ MeV and the three-body effective interaction in the $N_{\max}=14$ model space. In this calculation we obtained the best description of the ground state. The calculation of the elastic charge form factor in the impulse approximation can be directly compared to that presented in Fig. 2 of Ref. [36], performed using variational Monte Carlo (VMC) wave functions and the Argonne V14 NN potential. There, the minimum was obtained at $q \approx 3.55 \text{ fm}^{-1}$, while the experimental minimum is at $q \approx 3.2 \text{ fm}^{-1}$. The difference can be explained with the help of meson-exchange-current contributions. The elastic charge well with that obtained by the VMC wave functions. It is shifted further to higher q ; namely, we get the minimum at $q \approx 3.75 \text{ fm}^{-1}$. We note that a second

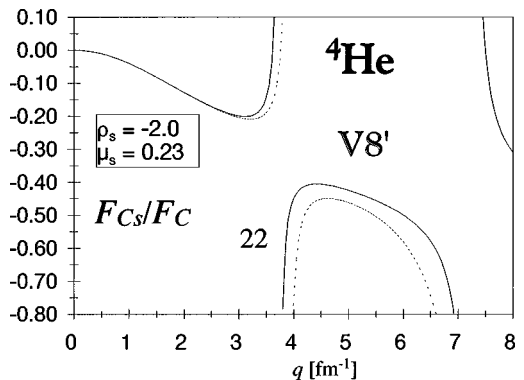


FIG. 13. The ratio of the elastic EM and strangeness charge form factors (solid line) and the EM and strangeness charge form factor corresponding to the transition to the first-excited 0^+0 state (dotted line) calculated in the impulse approximation using the three-body effective interaction derived from the Argonne V8' NN potential in the $N_{\max}=14$ model space and $\hbar\Omega=22$ MeV. Values of the strangeness radius $\rho_s = -2.0$ and the strangeness magnetic moment $\mu_s = 0.23$ were employed.

minimum appears in our calculated elastic charge form factor at $q \approx 7.25 \text{ fm}^{-1}$. The second minimum at a similar position was found in the VMC calculations presented in Ref. [38]. To examine the form factor dependence on $\hbar\Omega$, we repeated these calculations for different choices of the HO energy. In Fig. 11 we show the result obtained with $\hbar\Omega = 19 \text{ MeV}$. All other characteristics are the same as in the calculation of Fig. 10. The minimum here is shifted further to higher q ; we have it at $q \approx 3.85 \text{ fm}^{-1}$. The difference between the two results is rather small but still it shows that our calculation is not completely converged and, in particular, the description of the high-transferred-momentum part of the form factors requires the use of even larger model spaces than we employed. We note that the inelastic form factor has a stronger Ω dependence than the elastic form factor. As discussed in the previous subsection, convergence of the excited state has not been achieved in our calculations within the model spaces employed. Therefore, our calculated inelastic form factors must be taken with some degree of caution. Let us remark that, in addition to the transition form factor, we also computed the form factor of the first-excited 0^+0 state. That form factor was also evaluated in Ref. [17] in the resonating group method approach using the Bonn potential. Similarly as in that work, our calculated 0_2^+ form factor is almost an order of magnitude smaller than the ground-state form factor for a wide range of q . The first minimum is shifted in our calculation to larger q , more or less to the position of the transition form factor minimum, and the second minimum is shifted to smaller q compared to our ground-state form factor.

Our calculated elastic strangeness form factor and the inelastic EM charge form factor corresponding to the transition to the first-excited 0^+0 state are shown in Fig. 12. These results were obtained using the same wave functions as those used for calculations presented in Fig. 10; namely, we had $\hbar\Omega = 22 \text{ MeV}$, the model-space size characterized by $N_{\text{max}} = 14$, and the three-body effective interaction was employed. The elastic form factor can be compared with the impulse approximation VMC result of Fig. 3 in Ref. [36]. Similarly, as for the EM elastic form factor, our calculation compares well with VMC result. We note, however, the different value of strangeness magnetic moment used in Ref. [36] ($\mu_s = -0.2$).

Finally, in Fig. 13 we present the ratio of the EM and strangeness form factors from Figs. 10 and 12. The ratio of the elastic charge form factors is particularly interesting, as it can be experimentally obtained from the measurement of the parity-violating left-right asymmetry for scattering of polarized electrons from a ^4He target. Experiments of this type are now under preparation at TJNAF.

IV. CONCLUSIONS

In the present study we used equations for Faddeev amplitudes, antisymmetrized for three nucleons, to solve the shell-model problem for the four-nucleon system. We performed calculations in larger model spaces, up to a HO excitation of $14\hbar\Omega$ above the unperturbed ground state, than in any other shell-model study so far. The main motivation for the present work was to test the shell-model approach and the effective interactions that we want to apply to more com-

plex systems, e.g., p -shell nuclei, in particular. The effective interactions that we employed were derived from realistic NN potentials, i.e., the Reid93 and the Argonne V8'. In addition to the two-body effective interactions, we also computed the three-body effective interactions and demonstrated that their use significantly improves the convergence of the results.

Our calculations depend on the model-space size and on the HO frequency Ω . The effective interactions were constructed in such a way that in the large model-space limit the effective interactions approach the bare NN interaction. Thus our results should converge to the exact solutions. The dependence on the model-space size and Ω was investigated. We found quite different behavior of the ground state and the first-excited 0^+0 state. Our ground-state energy and point-nucleon radius results begin to converge and are close to or in agreement with those obtained by the GFMC method. For the first-excited 0^+0 state, our results, the point-nucleon radius, in particular, show large model-space and Ω dependence. This implies that significantly larger model spaces would still be needed in order to obtain the exact solutions. The nature of the 0_2^+ state is discussed in the literature [14,16]. The Coulomb interaction plays an important role in the description of this state. In the present calculations we did not include the isospin breaking. Our formalism is quite general, however, and allows the use of interactions that break the isospin symmetry. On the other hand, the calculated properties of the 0_1^- state show better convergence behavior. In the model spaces studied, we obtained lower excitation energy of the 0_1^- state than of the 0_2^+ state, contrary to experiment. The extrapolation of the model-space dependence of these two energies to larger model spaces shows, however, that the correct ordering of the states will be obtained. Apparently, the 0_2^+ state is associated with a radial excitation and, thus, it is more sensitive to the HO basis used in the expansion.

A sensitive test of our calculated wave functions is the computation of the charge EM and strangeness form factors. Our impulse-approximation results show little dependence on the NN potential and our best results are close to the corresponding form factors obtained using the VMC wave functions and the Argonne V14 NN potential. In particular, we observe both the first and the second minima in the elastic charge form factor in positions close to those obtained using the VMC calculations. In addition to the elastic charge form factors, we also evaluated the form factors for the transition to the 0_2^+ state in the impulse approximation.

In general, the energy scales of the bound $0s$ nucleons are significantly different from the scattering energies of the resonances. This difference can only be accounted for with a large N_{max} in our approach. Consequently, the results for the excited states and the transition form factors obtained within the limited model spaces of the present work should be taken with some caution. In the future we would like to apply the formalism, discussed in the present paper, to a more extensive study of the negative-parity states of ^4He . In particular, it is desirable to use still larger model spaces to investigate the excited-state convergence properties.

The most important result of the present work is, however, the successful use of the three-body effective interac-

tion. This three-body effective interaction can be computed for more complex nuclei as well and, in principle, used, after a transformation to an appropriate three-nucleon basis, in standard shell-model calculations. A more practical approach, however, is to make use of the three-body effective-interaction knowledge for the renormalization of the two-body effective interaction. Work in this direction is under way. In addition, the present formalism may be used to compute the four-body effective interaction for nuclei with $A > 4$. We plan to extend the shell-model Faddeev-like approach that we have successfully applied to three- and four-nucleon systems to systems with more than four nucleons,

using also a formalism of equations for components with lower degree of antisymmetry than the full wave function developed in Ref. [39].

ACKNOWLEDGMENTS

We thank Gintautas P. Kamuntavičius for useful comments concerning the symmetries present in Eqs. (9) and (18). This work was supported in part by NSF Grant No. PHY96-05192. P.N. also acknowledges partial support from a grant of the Grant Agency of the Czech Republic, No. 202/96/1562.

-
- [1] L. D. Faddeev, Zh. Eksp. Teor. Fiz. **39**, 1459 (1960) [Sov. Phys. JETP **12**, 1014 (1961)].
- [2] G. L. Payne, J. L. Friar, B. F. Gibson, and I. R. Afnan, Phys. Rev. C **22**, 823 (1980).
- [3] G. L. Payne, J. L. Friar, and B. F. Gibson, Phys. Rev. C **22**, 832 (1980).
- [4] C. R. Chen, G. L. Payne, J. L. Friar, and B. F. Gibson, Phys. Rev. C **31**, 2266 (1985).
- [5] J. L. Friar, G. L. Payne, V. G. J. Stoks, and J. J. de Swart, Phys. Lett. B **311**, 4 (1993).
- [6] A. Nogga, D. Hüber, H. Kamada, and W. Glöckle, Phys. Lett. B **409**, 19 (1997).
- [7] O. A. Yakubovsky, Sov. J. Nucl. Phys. **5**, 937 (1967).
- [8] W. Glöckle and H. Kamada, Phys. Rev. Lett. **71**, 971 (1993).
- [9] B. S. Pudliner, V. R. Pandharipande, J. Carlson, S. C. Pieper, and R. B. Wiringa, Phys. Rev. C **56**, 1720 (1997); R. B. Wiringa, Nucl. Phys. **A631**, 70c (1998).
- [10] M. Viviani, A. Kievsky, and S. Rosati, Few-Body Syst. **18**, 25 (1995).
- [11] D. C. Zheng, J. P. Vary, and B. R. Barrett, Phys. Rev. C **50**, 2841 (1994); D. C. Zheng, B. R. Barrett, J. P. Vary, W. C. Haxton, and C. L. Song, *ibid.* **52**, 2488 (1995).
- [12] P. Navrátil and B. R. Barrett, Phys. Rev. C **54**, 2986 (1996); **57**, 3119 (1998).
- [13] P. Navrátil and B. R. Barrett, Phys. Rev. C **57**, 562 (1998).
- [14] R. Ceuleneer, P. Vandeputte, and C. Semay, Phys. Rev. C **38**, 2335 (1988).
- [15] J. Carlson, V. R. Pandharipande, and R. B. Wiringa, Nucl. Phys. **A424**, 47 (1984).
- [16] A. Csòtò and G. M. Hale, Phys. Rev. C **55**, 2366 (1997).
- [17] H. M. Hofmann and G. M. Hale, Nucl. Phys. **A613**, 69 (1997).
- [18] M. Viviani, S. Rosati, and A. Kievsky, Phys. Rev. Lett. **81**, 1580 (1998).
- [19] F. Ciesielski and J. Carbonell, Phys. Rev. C **58**, 58 (1998); F. Ciesielski, J. Carbonell, and C. Gignoux, Nucl. Phys. **A631**, 653c (1998).
- [20] L. Trlifaj, Phys. Rev. C **5**, 1534 (1972).
- [21] E. P. Harper, Y. E. Kim, and A. Tubis, Phys. Rev. C **6**, 126 (1972).
- [22] W. Glöckle, *The Quantum Mechanical Few-Body Problem* (Springer-Verlag, New York, 1983).
- [23] V. A. Rudnev and S. L. Yakovlev, Phys. At. Nucl. **58**, 1662 (1995).
- [24] A. P. Yutsis, I. B. Levinson, and V. V. Vanagas, *Mathematical Apparatus of the Theory of Angular Momentum* (Israel Program for Scientific Translations, Jerusalem, 1962).
- [25] K. Suzuki and S. Y. Lee, Prog. Theor. Phys. **64**, 2091 (1980).
- [26] K. Suzuki, Prog. Theor. Phys. **68**, 246 (1982); K. Suzuki and R. Okamoto, *ibid.* **70**, 439 (1983).
- [27] V. G. J. Stoks, R. A. M. Klomp, C. P. F. Terheggen, and J. J. de Swart, Phys. Rev. C **49**, 2950 (1994).
- [28] A. G. M. van Hees and P. W. M. Glaudemans, Z. Phys. A **314**, 323 (1983).
- [29] J. P. Vary and D. C. Zheng, "The Many-Fermion-Dynamics Shell-Model Code," Iowa State University, 1994 (unpublished).
- [30] P. Navrátil, B. R. Barrett, and W. Glöckle, Phys. Rev. C **59**, 611 (1999).
- [31] K. Varga and Y. Suzuki, Phys. Rev. C **52**, 2885 (1995); K. Varga, Y. Ohbayasi, and Y. Suzuki, Phys. Lett. B **396**, 1 (1997).
- [32] D. C. Zheng, B. R. Barrett, J. P. Vary, and R. J. McCarthy, Phys. Rev. C **49**, 1999 (1994).
- [33] D. C. Zheng, B. R. Barrett, J. P. Vary, and H. Müther, Phys. Rev. C **51**, 2471 (1995).
- [34] S. C. Pieper (private communication).
- [35] M. M. Nagels, T. A. Rijken, and J. J. de Swart, Phys. Rev. D **17**, 768 (1978).
- [36] M. J. Musolf, R. Schiavilla, and T. W. Donnelly, Phys. Rev. C **50**, 2173 (1994).
- [37] B. Mueller *et al.*, Phys. Rev. Lett. **78**, 3824 (1997).
- [38] R. Schiavilla, V. R. Pandharipande, and D. O. Riska, Phys. Rev. C **41**, 309 (1990).
- [39] G. P. Kamuntavičius, Few-Body Syst. **1**, 91 (1986); Sov. J. Part. Nucl. **20**, 109 (1988).